Available online at www.sciencedirect.com
ScienceDirect
Atmospheric Environment 41 (2007) 6860–6871
ATMOSPHERIC ENVIRONMENT
www.elsevier.com/locate/atmosenv

Formation of particulate sulfur species (sulfate and methanesulfonate) during summer over the Eastern Mediterranean: A modelling approach

N. Mihalopoulos[a,*], V.M. Kerminen[b], M. Kanakidou[a], H. Berresheim[c], J. Sciare[d]

[a]*Environmental Chemical Processes Laboratory, Department of Chemistry, University of Crete, P. O. Box 2208, Voutes 71003 Heraklion, Greece.*
[b]*Finnish Meteorological Institute, Air Quality Research, Sahaajankatu 20E, FIN-00810, Helsinki, Finland*
[c]*Deutscher Wetterdienst (DWD), Meteorological Observatory, Hohenpeissenberg, Germany*
[d]*Laboratoire des Sciences du Climat et de l'Environnement, Gif-sur-Yvette, France*

Received 5 January 2007; received in revised form 15 April 2007; accepted 16 April 2007

Abstract

To improve our understanding of the mechanisms of particulate sulfur formation (non sea-salt sulfate, nss-SO_4^{2-}) and methanesulfonate (MS_x used here to represent the sum of gaseous methanesulfonic acid, MSA, and particulate methanesulfonate, MS^-) in the eastern Mediterranean and to evaluate the relative contribution of biogenic and anthropogenic sources to the S budget, a chemical box model coupled offline with an aerosol–cloud model has been used.

Based on the measurements of gaseous dimethyl sulfide (DMS) and methanesulfonic acid (MSA) and the MSA sticking coefficient determined during the Mediterranean Intensive Oxidant Study (MINOS) experiment, the yield of gaseous MSA from the OH-initiated oxidation of DMS was calculated to be about 0.3%. Consequently, MSA production from gas-phase oxidation of DMS is too small to explain the observed levels of MS^-. On the other hand, heterogeneous reactions of dimethyl sulfoxide (DMSO) and its gas-phase oxidation product methanesulfinic acid (MSIA) can account for most of the observed MS^- levels. The modelling results indicate that about 80% of the production of MS^- can be attributed to heterogeneous reactions.

Observed submicron nss-SO_4^{2-} levels can be fully explained by homogeneous (photochemical) gas-phase oxidation of sulfur dioxide (SO_2) to sulfuric acid (H_2SO_4), which is subsequently scavenged by (mainly submicron) aerosol particles. The predominant oxidant during daytime is hydroxyl radical (OH) showing very high peak levels in the area during summer mostly under cloudless conditions. Therefore, during summer in the east Mediterranean, heterogeneous sulfate production appears to be negligible. This result is of particular interest for sulfur abatement strategy. On the other hand only about 10% of the supermicron nss-SO_4^{2-} can be explained by condensation of gas-phase H_2SO_4, the rest must be formed via heterogeneous pathways.

Marine biogenic sulfur emissions contribute up to 20% to the total oxidized sulfur production (SO_2 and H_2SO_4) in good agreement with earlier estimates for the area.

Keywords: Sulfate; Methanesulfonate; Summer time; Eastern Mediterranean; Modelling

*Corresponding author. Fax: +30 2810 545001.
E-mail address: mihalo@chemistry.uoc.gr (N. Mihalopoulos).

1352-2310/$ - see front matter © 2007 Elsevier Ltd. All rights reserved.
doi:10.1016/j.atmosenv.2007.04.039

1. Introduction

Particles can play an important climatic role by scattering solar radiation and acting as cloud condensation nuclei (CCN), thus influencing the Earth's albedo and climate (IPCC, 2001). However, due to the spatial and temporal heterogeneity of aerosol occurrence and properties, an increased effort at characterizing tropospheric aerosols is needed to reduce the uncertainty in the aerosol forcing estimate (Schwartz and Andreae, 1996). Recent model studies reproduced satellite observations and demonstrated the key role of three major components of aerosols in regions surrounding the Mediterranean basin (sulfate, black carbon, and dust; Sciare et al., 2003).

In the eastern Mediterranean atmosphere, sulfate contributes more than 50% to the submicron aerosol mass (Bardouki et al., 2003a,b; Sciare et al., 2005), a situation not observed over Western Europe and over North America. Therefore, understanding the mechanisms of the formation of particulate sulfur which occurs mainly as non-sea-salt sulfate (nss-SO_4^{2-}) and methanesulfonate (MS^-) is of great concern with respect to reducing the relative contribution from anthropogenic sources in the eastern Mediterranean.

Sulfur has both anthropogenic and biogenic sources. Kouvarakis et al. (2002) by comparing the ocean emitted biogenic sulfur (predominantly dimethyl sulfide—DMS) with the total deposited S, suggested that the contribution from biogenic sources can account for up to 26% during summer. Therefore, DMS oxidation can explain a non-negligible part of the high nss-SO_4^{2-} values observed during summer in several places in the eastern Mediterranean area (Kubilay et al., 2002). The MINOS (Mediterranean Intensive Oxidant Study) campaign conducted on Crete Isl. in July–August 2001 (with simultaneous airborne measurements across the Mediterranean basin), provides the first comprehensive dataset to understand the factors controlling the particulate sulfur formation in the area (Bardouki et al., 2003a). During this campaign, intensive measurements of gaseous DMS, DMSO, sulfur dioxide (SO_2), sulfuric acid (H_2SO_4), methanesulfonic acid (MSA), and of size resolved particulate SO_4^{2-} and MS^- have been performed in conjunction with measurements of oxidants including OH (Berresheim et al., 2003; Bardouki et al., 2003a) and NO_3 (Vrekoussis et al., 2004) radicals.

The aim of the present work is to go a step farther compared to Bardouki et al. (2003a) and to address key questions related to the S cycle in the area via analysis of this extensive dataset. In particular, we investigate (i) the importance of the gas phase versus heterogeneous reactions leading to MS^- and nss-SO_4^{2-} formation in the eastern Mediterranean and (ii) the relative contributions from biogenic and anthropogenic sources to the S budget. For this we combine sulfur dioxide, hydroxyl radical, sulfate and rate constant of condensational sink (k_{cs}) observations with the sulfate size segregated measurements and zero-dimensional model results.

2. Experimental

2.1. Location and measurements

All measurements reported here have been performed at Finokalia (35°24′N, 25°60′E), a remote location on the northern coast of Crete Isl., Greece. Details on area and meteorological conditions encountered year-round are given by Mihalopoulos et al. (1997). The MINOS experiment has been conducted from 28 July to 22 August 2001 and the following key species have been measured:

- DMS with an average sampling interval of 1 h (490 measurements by gas chromatography equipped with flame photometric detector GC–FPD).
- DMSO with an average sampling step of 3 h (201 measurements by GC–FPD).
- Gaseous SO_2 and bulk aerosol (SO_4^{2-} and MS^-) samples collected simultaneously with DMSO (226 measurements by ion chromatography). Details of the analytical techniques used are given by Kouvarakis et al. (2002). All these compounds and associated measurements have been reported by Bardouki et al. (2003a).
- H_2SO_4, MSA and OH concentrations in the gas phase were measured by Berresheim et al. (2003; see details on instrument description and results) using chemical ionization mass spectrometry (CIMS).
  Meteorological parameters like temperature, humidity, wind speed and direction were measured continuously by an automated meteorological station.
- Size-segregated aerosols were collected on a 3-day basis at the Finokalia marine boundary layer sampling station using a 11-stage micro-orifice uniform deposit impactor (MOUDI, MSP

Corporation) operating with 47-mm diameter nuclepore polycarbonate and Teflon filters, for mass and ions (Sciare et al., 2005).

2.2. Selected period and model descriptions

2.2.1. Modelling period

Our modelling effort has been limited to the period 14–18 of August, for two reasons: (i) During this period, air masses were originating from the N, NE sectors, typical wind pattern during summertime in the area and no significant changes have occurred in the transport pathways. Wind speed ranged from 4 to 12 m s^{-1} (mean value of 8 m s^{-1}) and air temperature ranged from 22.6 to 25.4 °C (mean value 23.6 °C). (ii) There is a satisfactory amount of observations available from this period, on the major components of the S cycle, i.e. of oxidants (OH and NO_3), aerosol precursors, and intermediate and final S oxidation products (Table 1).

To achieve our aims, a chemical box model and an aerosol box model have been used. For the present study, the chemical box model is used to evaluate the contribution to the S budget in the area of anthropogenic relative to biogenic sources and to provide indications on the importance of heterogeneous and gas-phase reactions for the sulfur cycle. In addition, the aerosol model complements the analysis and describes explicitly the gas–aerosol partitioning. Furthermore, it addresses the role of heterogeneous and gas-phase reactions on the MS^- and nss-SO_4^{2-} formation in both coarse and fine aerosol size fractions. Below the two models and the initial conditions used are briefly presented.

2.2.2. Chemical box model description

The commercially available software FACSIMILE (Curtis and Sweetenham, 1988), which uses automatic time step selection and error control, was used to solve the differential equations with a high accuracy required for chemistry studies. The chemistry model is a condensed chemical mechanism (about 300 chemical reactions and 140 chemical species). The chemical model is able to simulate marine boundary layer photochemistry of ozone, water vapor, nitrogen oxides, carbon monoxide and volatile organics (Tsigaridis and Kanakidou, 2002; Vrekoussis et al., 2004) as well as the gas-phase chemistry of sulfur. In addition to background $O_3/NO_x/OH/CO$ and CH_4 chemistry, it also takes into account the oxidation chemistry of C_1–C_5 hydrocarbons including isoprene (Tsigaridis and Kanakidou 2002; Vrekoussis et al., 2004) and biogenic sulfur oxidation mechanisms (Sciare et al., 2000). Oxidation of volatile organic compounds (VOC) by all three major oxidants (O_3, OH and NO_3) is considered when applicable.

Table 1
Observed mean, median and range of mixing ratios of DMS and the other gaseous and particulate S species during the modelled period 14-18/8 (n = number of data)

Compound	N	Mean	Median	Range
(pmol mol^{-1})				
DMS	113	16.6	14	(1.8–67.6)
DMSO	40	2.2	1.7	(0.08–8.5)
MS^-	45	11.9	11.3	(5.3–19.4)
SO_2	45	738	910	(306–2023)
nss-SO_4^{2-}	45	1186	1300	(557–2000)
(molecules cm^{-3})				
MSAg	965	7.4×10^4	7.4×10^4	$(2.2 \times 10^4$–$1.5 \times 10^5)$
H_2SO_4g	154	7.8×10^6	4.1×10^6	$(1.5 \times 10^5$–$3.7 \times 10^7)$

The mean values for MSA and H_2SO_4 have been calculated using hourly data.

2.2.2.1. DMS oxidation chemistry. The applied version of the chemical model focuses on the gas-phase reactions of SO_2 and DMS, while the gas–aerosol partitioning of gaseous H_2SO_4, MSA and DMSO is simply parameterized based on a condensation sink driven by a pseudo-first order rate constant k_{cs} using values reported by Bardouki et al. (2003a). The adopted DMS chemistry scheme takes into account DMS oxidation by OH and NO_3 radicals and is an update Sciare et al. (2000). This update is given in Table 2 and is based on Atkinson et al. (2004) and a recent review on DMS chemistry by Barnes et al. (2006).

For SO_2, in-cloud oxidation was not considered due to the absence of clouds during the whole campaign; however, SO_2 oxidation on sea-salt particles is taken into account. Dry deposition (V_d), which is species specific, is taken into account in the model. An entrainment velocity of 0.168 cm s^{-1} has been also adopted (Sciare et al., 2000). The chemical box model results do not show any sensitivity to this velocity for values between 0.1 and 0.2 cm s^{-1}.

2.2.3. Aerosol model description

The aerosol model used in the simulations is an updated version of a box model used earlier by Kerminen and co-workers (Kerminen et al., 2000;

Table 2
Reduced reaction scheme for DMS initiated oxidation by OH and NO_3 radicals used during this study

Reaction rates	DMS oxidation scheme – reactions
$R_{OHDMSab} = 1.13E{-}11 \exp(-253/T)$	Reaction with OH via H abstraction $DMS + OH \rightarrow 0.997\ (SO_2 + CH_3O_2 + HCHO) + 0.003\ (MSA + HCHO)$
$R_{OHDMSad} = k_1/k_2$ $k_1 = 1.7E{-}42 \exp(7810/T)[O_2]$ $k_2 = 1 + 5.5E{-}31 \exp(7460/T)[O_2]$	Reaction with OH via OH addition $DMS + OH \rightarrow DMSO$
$R_{NO_3DMS} = 1.9E-13 \exp(500/T)$	Reaction with NO_3 via H-abstraction $DMS + NO_3 \rightarrow SO_2 + HNO_3 + CH_3O_2 + HCHO$
$R_{OHDMSO} = 9.E{-}11$ $R_{OHMSIA} = 9.E{-}11$	DMSO and MSIA gas phase chemistry $DMSO + OH \rightarrow MSIA + CH_3O_2$ $MSIA + OH \rightarrow CH_3O_2 + SO_2 + H_2O$
$k_{SO_2\_SSA} = 8.7E-6$ k_{cs1} (*) k_{cs2} (*)	Heterogeneous reactions and phase changes $SO_2 \rightarrow SO_4^{=}$ (coarse) $H_2SO_4 \rightarrow SO_4^{=}$ (fine) $MSA \rightarrow MS^-$
$k_{DMSOaq} = 1E{-}10$ [OH] $1.5 \times k_{DMSOaq}$	DMSO aqueous phase chemistry $DMSO \rightarrow MS^-$ $MSIA \rightarrow MS^-$
$k_{OHSO_2} = k_1/(1. + k_1/k_2) * 0.5 * *(1./(1. + \log 10(k_1/k_2) * *2))$ $k_1 = 3E{-}31(T/300)**(-3.3)*[air]$ $k_2 = 1.5E{-}12$	SO_2 chemistry $SO_2 + OH \rightarrow HSO_3$
$k_{SO_2HO_2} = 1.E-18$	$SO_2 + HO_2 \rightarrow SO_3 + OH$
$k_{SO_2MO_2} = 5.E-17$	$SO_2 + CH_3O_2 \rightarrow HCHO + HO_2 + SO_3$
$k_{HSO_3O_2} = 1.E-11 \exp(-1000/T)$	$HSO_3 + O_2 \rightarrow SO_3 + HO_2$
$k_{SO_3H_2O} = 2.4E-15$	$SO_3 + H_2O \rightarrow H_2SO_4g$

Kerminen, 2001; Kerminen and Leck, 2001) to investigate both aerosol–trace gas and aerosol–cloud interactions. Briefly, the Lagrangian model box follows an air parcel in the boundary layer. The box interacts with the free troposphere via entrainment and with the surface via dry deposition and emissions of both aerosols and trace gases. The model is capable of simulating all basic aerosol processes, including (parameterized) nucleation, condensational growth of aerosol particles by both non-volatile and semi-volatile trace gases, coagulation, cloud droplet activation and deactivation, as well as aqueous-phase reactions taking place in hygroscopic aerosol particles or in cloud droplets.

In the model, the aerosol number size distribution is prescribed by a specified number of modes that may overlap with each other. Depending on the application, each mode is further divided into 10–100 sizes bins. The model is initialized by assuming that the modes are log-normally shaped and that aerosol particles in the same mode have the same chemical composition. During the simulation, various aerosol processes modify the "dry" diameter, chemical composition and number concentration of particles in every size bin. The "wet" diameter of particles in each size bin is calculated based on the particle hygroscopic properties in that size bin.

The concentrations of gaseous compounds interacting with aerosol particles or cloud droplets have been taken from measurements. The condensing compounds treated by the aerosol model are sulfuric acid (H_2SO_4), methanesulfonic acid (MSA), and both a generic non-volatile and semi-volatile organic compound. In the present simulations, initial concentrations of condensable organic vapors were set to zero. The simulated chemical components in the aerosol phase include sulfate, sea-salt, dust, carbonaceous matter and water.

Sea-salt concentration was calculated as 3.25 times the sodium concentration (equivalent to the

Na: total sea salt mass ratio in fresh sea-salt particles; e.g. Seinfeld and Pandis, 1998). The remaining supermicron mass was assumed to be dust. These two compounds account for more than 80% of the total coarse mass fraction (Sciare et al., 2005).

2.3. Simulation setup

2.3.1. Chemistry model simulations

Observed hourly mean values of ozone, photolysis rates of nitrogen dioxide (JNO_2) and ozone (JO^1D) and carbon monoxide are used as input to the model that was also forced every 5-min by the geometric hourly mean of NO_2 observations (Vrekoussis et al., 2004). Isoprene, ethene, propene, formaldehyde, acetaldehyde, ethane, propane and butane mixing ratios are kept equal to 7, 100, 50, 1000, 100, 1000, 260 and 120 pptv, respectively, according to observations during the MINOS campaign (Gros et al., 2003). Aerosol surface concentrations obtained during the campaign (Bardouki et al., 2003a) are used to calculate the heterogeneous removal rates as described by Tsigaridis and Kanakidou (2002). Diurnal mean DMS levels were used to account for the DMS emitted by the sea and its impact on the marine boundary layer chemistry. Initial concentrations of hydrogen peroxide (495 pptv), methane (1.8 ppmv) and particulate nitrate (25 nmol m^{-3}) are applied.

Several simulations have been performed by varying the MSA yield from DMS oxidation by OH via H abstraction between 0.2% and 0.5% as suggested by Bardouki et al. (2003a) to investigate the related uncertainty. Finally, to evaluate the biogenic sulfur contribution to the H_2SO_4 levels an additional simulation has been performed with the initial SO_2 concentrations set to zero. Each simulation was run for the selected period from 14 to 18 August 2001 (see Section 2.2.1). The first 2 days have been used as spin-up time and the last 3 days have been analysed for the present study.

2.3.2. Aerosol model simulations

The aerosol model was run with an aerosol size distribution consisting of three log normal modes: an accumulation mode and supermicron sea-salt and dust modes. No Aitken or nucleation mode was considered, since the study focuses on simulating the mass size distributions of different aerosol components and very small fraction of the simulated components resides below the accumulation mode size range. During the model initialization, the accumulation mode was assumed to consist of carbonaceous matter only, whereas the sea-salt mode was assumed to contain 99% of sea salt and 1% of organic matter. In the dust mode, no sea-salt, carbonaceous matter or sulfur compounds were assumed to be present. None of the modes contained initially sulfate or MSA.

Only the accumulation and sea-salt modes were assumed to contain water. When calculating the water uptake of the accumulation mode, 15% of the carbonaceous matter was assumed to behave as ammonium sulfate. This choice, while somewhat arbitrary, is consistent with the measured hygroscopic properties of particles containing various organic aerosol mixtures (Malm et al., 2005). The dry densities of accumulation mode particles, being mixtures of sulfate and carbonaceous matter, were assumed to be 1.5 g cm^{-3} during the whole simulation period (Turpin and Lim, 2001). The dry densities of particles in the sea-salt and dust modes were set equal to 2.16 and 2.65 g cm^{-3}, respectively (Tegen and Fung, 1994; Moldanova and Ljungström, 2001).

The initial modal parameters (particle number concentration, mean diameter and geometric standard deviation) of the three modes were constrained based on number size distribution observations (Bardouki et al., 2003a). For sea-salt and dust modes, these constraints were the impactor-based sea-salt and dust concentrations in the size range 1–10 μm and the mass mean diameters of these components. The geometric standard deviation of these two modes was set equal to 1.7. For the accumulation mode, the corresponding constraints were the impactor-based total submicron mass concentration and mass mean diameter. An important further constraint was that the condensation sink of sulfuric acid, being dependent on all the three modes, was approximated by that obtained by Bardouki et al. (2003a) based on observations and mass balance calculations.

Of aerosol processes, nucleation, coagulation and cloud processing were neglected during the simulations. The omission of nucleation can be considered justified because no sign of this process was observed during the considered period and because nucleation has in general little influence on the aerosol mass size distribution. Coagulation decreases the number concentration of accumulation mode particles, but its influence on the aerosol mass size distribution is expected to be negligible.

Particle dry deposition onto the ocean surface was calculated according to the model of Slinn and Slinn (1980) using the measured average surface wind speed of $8\,m\,s^{-1}$. An entrainment velocity of $0.15\,cm\,s^{-1}$ was assumed. Since the concentrations of both accumulation mode and larger particles were probably significantly lower in the free troposphere than in the boundary layer, entrainment was treated as a sole sink of particles from our model box. The replacement of aged sea-salt particle by fresh ones was taken care by keeping the sea-salt particle concentration constant during the simulation and by allowing dry deposition and entrainment to affect only the secondary aerosol components (non-sea-salt sulfate and MS^-) present in sea-salt particles.

Important parameters in simulating particulate sulfate and MSA production are the mass accommodation coefficients of gaseous H_2SO_4 and MSA on particle surfaces. Based on various laboratory and field studies, the mass accommodation coefficient of H_2SO_4 is probably in the range 0.5–1 (Jefferson et al., 1997; Pöschl et al., 1998), whereas that of MSA is considerably lower (De Bruyn et al., 1994). Here, mass accommodation coefficients of 1 and 0.1 for H_2SO_4 and MSA, respectively, were assumed.

Two base-case simulations were performed, termed the DRY and WET simulations. In the DRY simulation, only condensation of gaseous H_2SO_4 and MSA were allowed to form particulate sulfate and MS^-. In the WET simulation, we included the oxidation of SO_2 to sulfate by O_3 in sea-salt particles, as well as the oxidation of DMSO to MSA by OH in both accumulation mode and sea-salt particles. The liquid-phase concentrations of SO_2, DMSO, O_3 and OH were calculated based on their (effective) Henry's law constants (Herrmann et al., 2000). Unfortunately, the Henry's law constant of DMSO is not very well known. Lee and Zhou (1994) estimated a lower limit of $10^6\,M\,atm^{-1}$ for this constant, whereas larger values of up to $10^7\,M\,atm^{-1}$ have been assumed in more recent model simulations (Campolongo et al., 1999; Zhu et al., 2006). In our WET simulations, we conservatively chose a value of $10^6\,M\,atm^{-1}$ for this constant. The liquid-phase rates of the reactions of SO_2 with O_3 and of DMSO with OH were taken from Hoffman (1986) and Zhu et al. (2006), respectively. For simplicity, pH of wet aerosols was kept fixed during the simulations.

The model simulations covered a total of 120 h, starting from 00:00 on August 14 and ending at 24:00 on August 18. During the simulations, the ambient temperature and relative humidity and the gas-phase concentrations of H_2SO_4, MSA, DMSO, SO_2 and OH were taken directly from measured 1-h average data. The initial modal parameters of the accumulation, sea-salt and dust modes were chosen iteratively in such a way that after repeating the 120-h simulation a sufficient number of times, the simulated modal mass concentrations and mean diameters, as well as average condensation sink of sulfuric acid, were very close to those observed. The second impactor sample was chosen as a basis for this comparison. The first impactor sample was used to get additional information on how stable the concentrations of different aerosol species were during the simulation period.

3. Results and discussion

3.1. Chemistry simulation results

Vrekoussis et al. (2004) have shown that the model satisfactorily simulates the daytime variation and the absolute concentrations of OH radicals although overall, it underestimates the observations of OH radical by about 8% and captures the order of magnitude of the NO_3 observations within the range of their variability. Therefore, it is able to simulate reasonably well both the gas-phase daytime and nighttime oxidation of DMS and SO_2 in the area. The sulfur simulations are analysed hereafter.

3.1.1. MSA

Fig. 1a compares the simulated MSA levels to the measured ones (16–18th of August 2001) for the base-case simulation. This simulation has been performed using the measured DMS and OH levels. Since during night the observed MSA concentrations were below the detection limit, no MSA production from the DMS reaction with NO_3 is assumed in the model. The condensation sink for MSA changed daily based on the values reported by Bardouki et al. (2003a). The simulated MSA levels compare well with the modeled one only when the yield of MSA from DMS oxidation by OH radicals is set to 0.003. Sensitivity studies have been performed by changing the yield from 0.2 to 0.5% and the best fit is obtained when the value of 0.3% is used.

3.1.2. H_2SO_4

Fig. 1b compares the simulated H_2SO_4 levels to the measured ones. The simulation has been

performed using the measured OH and SO_2 levels. During the simulation, the condensation sink for H_2SO_4 changed from a day to another based on the values reported by Bardouki et al. (2003a). The simulated H_2SO_4 levels compare very well with the observations (slope = 0.87, $r^2 = 0.8$).

Based on a yield of MSA from DMS oxidation of 0.3% that has been shown suitable for the studied area based on MSA observations and simulations, the H_2SO_4 levels originating from the DMS oxidation alone can be simulated. These levels are shown in Fig. 1c and correspond to the contribution of the biogenic S to the total measured H_2SO_4 and SO_4^{2-} levels. The simulation has been performed using the same conditions with the previously reported Fig. 1b. The simulated biogenic H_2SO_4 levels range between 5% and 20% of the measured ones indicating a biogenic S contribution in good agreement with the mean values reported during summer by Kouvarakis et al. (2002). Based on aerosol data collected under pure marine conditions during an oceanographic cruise, Bates et al. (1992) proposed a relationship between the biogenic MSA/nss-SO_4^{2-} ratio and air temperature. Thus the relative contributions of biogenic and anthropogenic sulfate could be estimated by comparing the

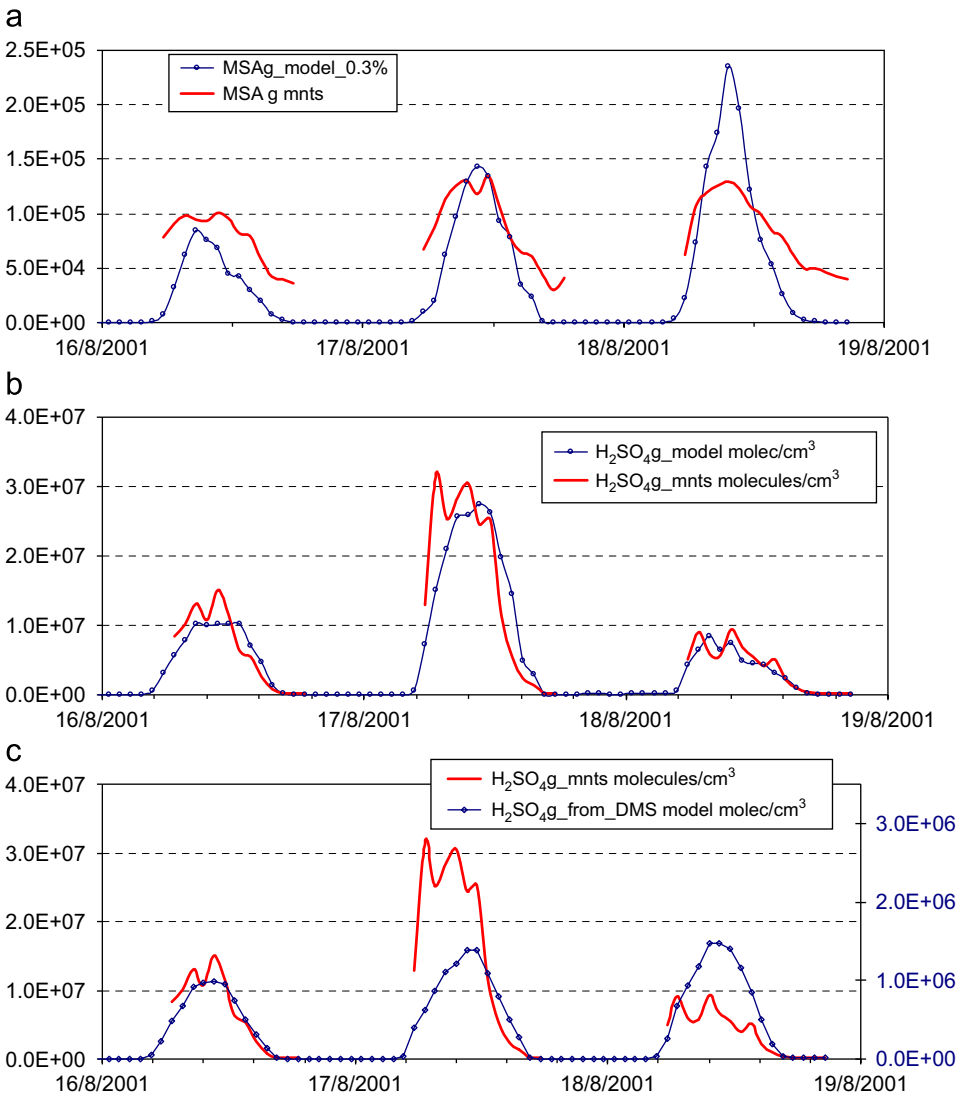

Fig. 1. Comparison between the modeled and measured (a) MSA, (b) H_2SO_4, and (c) biogenic or DMS derived H_2SO_4 (right axis) versus total measured H_2SO_4 (left axis).

MSA/nss-SO_4^{2-} ratio calculated by the Bates et al. (1992) equation, with that derived from the MSA and nss-SO_4^{2-} field observations. This procedure leads to an estimate of the biogenic sulfur fraction in the range of 6–38% (mean value of $17 \pm 8\%$) in quite good agreement with the 5–20% derived from our box model calculation.

As shown in Table 2, the gas-phase oxidation of MSIA by OH has been assumed to form SO_2 at a 100% yield based on Kukui et al. (2003). That work, however, performed in N_2 might not be transferable to the real atmosphere. Indeed, preliminary results from photoreactor studies suggest that under atmospheric conditions the SO_2 yield could be as low as 20% (Barnes et al., 2006). Under such conditions if the other reaction products do not finally lead to SO_4^{2-} formation, the here reported values of biogenic contribution are quasi ''upper limits''. Although the biogenic contribution to sulfate levels estimated by our box model has been successfully checked against the independent method of Bates et al. (1992), an additional sensitivity test has been performed. For this, the reaction of MSIA + OH was supposed to only partially lead to SO_2 with a yield of 20% as proposed by Barnes et al. (2006) while the remaining ca. 80% was supposed to form sulfur compounds that do not lead to SO_4^{2-} formation (e.g. $DMSO_2$). Since both DMSO and MSIA, the main products of the addition channel of DMS oxidation by OH, are drastically taken up by existing aerosols, the importance of gaseous phase reactions with OH radicals is limited. Therefore, the above assumption on SO_2 yield is changing our initial estimates of biogenic S production by only 5% and does not alter the conclusions of the paper.

3.1.3. MS^-

Since the gaseous MSA levels are reasonably simulated, it is interesting to compare the modelled levels of particulate MS^- to the measured ones. It is clear from Fig. 2a that simulated MS^- levels are at least an order of magnitude lower than the observed ones indicating that gas-particle conversion of MSA is of minor importance for measured MS^- levels. MSA may re-evaporate into the gas phase at low relative humidities (Bardouki et al., 2003a); however, such conditions did not occur during the simulation period and they are quite rare during summer in the area. The simulation has been repeated by assuming heterogeneous reactions of DMSO and MSIA (Table 2) following the recommendations by Barnes et al. (2006) and the results are depicted in Fig. 2b. It is clear that inclusion of heterogeneous reactions of DMSO and MSIA can bring a better agreement between the observed and simulated values of MS^-. The levels of MS^- and nss-SO_4^{2-} are also simulated using the more detailed aerosol model and the results are discussed in the next section.

3.2. Aerosol simulation results

Predicted concentrations of non-sea-salt sulfate (nss-SO_4) and methane sulfonate (MS^-) in the DRY base-case simulation, together with the corresponding measured concentrations, are shown in Table 3. Since the initial aerosol size distribution used in the simulations was constrained against the second impactor sample, the model predictions should in principle be compared with measurements from the same impactor sample. The success of this comparison depends, however, on how representative the locally measured trace gas and aerosol concentrations are of those experienced by the measured aerosol masses during their transport to our measurement site. Potential uncertainties arising from this problem can be estimated by looking at differences in aerosol concentrations between the first and second impactor sample. Table 3 suggests that these uncertainties are 25–30% for submicron nss-SO_4, about a factor of two for supermicron nss-SO_4 and up to a factor of three for MS^-.

Based on the two impactor samples in Table 3, the DRY simulation seems to be successful in predicting the concentration of submicron nss-SO_4 in measured air masses. This suggests that within observational uncertainties, condensation of gaseous sulfuric acid alone is able to explain the formation of submicron nss-SO_4 during the period considered here. Further support for this conclusion is obtained from aerosol mass size distributions: the ratio between the mass mean diameter of submicron nss-SO_4 and that of submicron particulate mass was below unity (in the range 0.7–0.8) and very similar in both the second impactor sample and in the model simulation. The corresponding ratio would be expected to be close to unity if reactions taking place in wet aerosol particles, rather than condensation, were the main formation route of submicorn nss-SO_4.

The simulated supermicron nss-SO_4 concentration is too low by roughly an order of magnitude, suggesting that reactions taking place either in wet

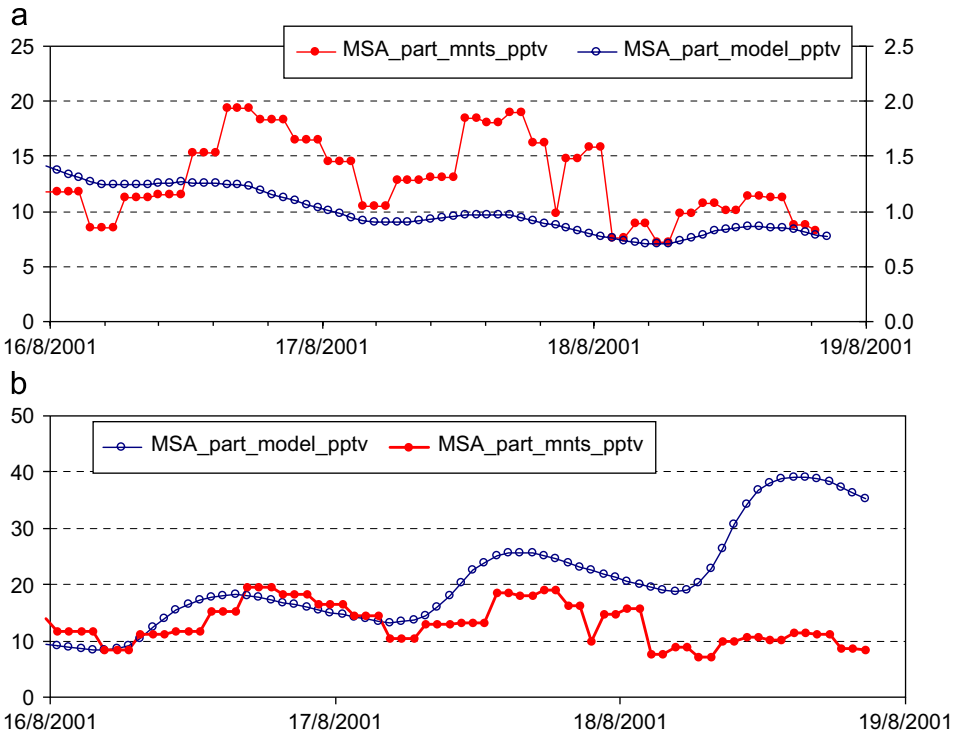

Fig. 2. Comparison between the modeled and measured MS^- by considering (a) only gas-phase chemistry (for observations see axis to the left and for model results axis to the right) and (b) gas phase and heterogeneous chemistry. Units are pptv.

Table 3
Measured and simulated (DRY base case) concentrations (ng/m^3) of aerosol species

Compound	First impactor	Second impactor	Simulated
nss-SO_4 (<1 μm)	4290	3200	3900
nss-SO_4 (1–10 μm)	640	340	38
MSA (<1 μm)	48	17	5.6
MSA (1–10 μm)	3	–	0.2
Sea-salt (1–10 μm)	4000	2400	–
Dust (1–10 μm)	14,700	9800	–

Note that simulated sea-salt and dust concentrations were constrained to match the observations.

sea-salt particles or on the surface of dust particles were the dominant source of supermicron nss-SO_4. In the case of MSA, the simulated concentration is too low by a factor of 3–10 depending on whether we rely on the first or second impactor sample. Two potential reasons for this underprediction can be identified: either the mass accommodation coefficient of gaseous MSA on particle surfaces is substantially higher than assumed here or, similar to supermicron nss-SO_4, particulate MSA was mainly formed by heterogeneous pathways. Below we have a more detailed look at heterogeneous nss-SO_4 and MSA production. The role of mass accommodation coefficient will be discussed in Section 3.3.

The most likely heterogeneous nss-SO_4 formation pathway in a cloud-free marine boundary layer is the oxidation of SO_2 by O_3 in wet sea-salt particles (e.g. Sievering et al., 2004). We made a number of simulations by including this reaction and by varying the pH of sea-salt particles. We found that the SO_2–O_3 reaction cannot explain the observed supermicron nss-SO_4 concentration unless the sea-salt pH is >5.5 during the whole simulation period. Such pH values are much higher than what have been measured or modelled in the case of aged supermicron sea-salt aerosols in the marine boundary layer (Keene et al., 2004). The pH of freshly emitted sea-salt particles is usually above 7, which results in very rapid sulfate formation until the alkalinity of these particles has been consumed e.g Chameides and Stelson, 1992). We calculated that

the amount of supermicron sulfate that can be produced due to the alkalinity present in natural sea water was $<10\,ng\,m^{-3}$, or $<3\%$ of the measured level of supermicron nss-SO_4. There are mechanisms that may enhance the alkalinity of sea-salt particles compared to that of sea water (Sievering et al., 2004), but their potential role cannot be estimated without more detailed information on the composition of sea-salt particles and the associated chemistry. Another pathway to explain the non simulated part of supermicron nss-SO_4 is reaction on dust particles which account for the majority of supermicron mass (Table 3).

When including the aqueous DMSO–OH reaction, the simulated particulate MS^- concentration increases from 6 to $29\,ng\,m^{-3}$, with $>80\%$ of it residing in the submicron size range, and thus better fits with measured values reported in Table 3. Even higher MSA concentrations would have been obtained if the Henry's law constant of DMSO was set larger than what was assumed in our base-case simulation. It should be noted that our simulations did not account for potential mass transport limitations associated with the gas–aerosol partitioning of DMSO and OH. By using the theoretical framework of Shi and Seinfeld (1991), it may be estimated that mass transport effects were probably negligible for submicron particles but they might slow down the DMSO–OH reaction taking place in wet sea-salt particles, especially if the Henry's law constant of DMSO exceeds $10^6\,M\,atm^{-1}$.

3.3. Sensitivity studies

It is clear that many of our model parameters are not well constrained, causing uncertainties in the simulation results. Two such parameters are the mixed layer height and entrainment velocity, both being dependent on various meteorological parameters. Changing the mixed layer height by $\pm10\%$ changed the simulated nss-SO_4 and MSA concentrations by about $\pm3\%$. The corresponding changes were $\pm8\%$ if an entrainment velocity of 0.1 or $0.2\,cm\,s^{-1}$ was used. Particle dry deposition velocity depends on the wind speed that varied from 5 to $11\,m\,s^{-1}$ during the simulation period. The resulting uncertainty in simulated nss-SO_4 and MSA concentrations was $<2\%$ for the submicron size range and $<10\%$ for the supermicron size range.

Transportation of H_2SO_4 and MSA from gas to the aerosol phase by condensation is dependent on the mass accommodation coefficient of these compounds with respect to particle surface deposition. Reducing the mass accommodation coefficient of H_2SO_4 from unity had practically no effect on our simulation results as long as the initial aerosol size distribution was modified in such a way that the condensation sink of H_2SO_4 remained close to the observed values. Contrary to this, the mass accommodation coefficient of MSA had a large impact on its simulated concentration in the aerosol phase. An accommodation coefficient of 0.3 for MSA was enough to produce the observed MSA concentration of $17\,ng\,m^{-3}$ by condensation alone. Assuming a unity as accommodation coefficient resulted in a concentration of $45\,ng\,m^{-3}$ for particulate MSA.

Long-term measurements in Finokalia indicate that the aerosol size distribution may have a more fine structure (more modes) than what we assumed in our base-case simulations (Gerasopoulos et al., 2007). We repeated the aerosol model simulations by varying the modal shape of the initial particle number size distribution. In the submicron size range, this procedure had relatively little influence on simulated nss-SO_4 and MSA concentrations as long as the condensation sink was kept fixed. Much larger uncertainties up to 50% for submicron nss-SO_4 and MSA were obtained when we tried to constrain our initial particle number size distribution just by relying on the measured submicron mass size distribution without any knowledge about the condensation sink. In the supermicron size range, uncertainties in simulated nss-SO_4 and MSA concentrations due to the variability in the aerosol size distribution were found to be in the range 30–40%. We conclude that there was roughly a 30% uncertainty in simulated nss-SO_4 and MSA concentrations related to how accurately the pre-existing aerosol number size distribution was known during the simulation period.

In the supermicron size range, uncertainties in simulated nss-SO_4 and MSA concentrations due to the variability in the aerosol size distribution were found to be in the range of 30–40%.

In the absence of rain, the lifetime of accumulation mode particles in the marine boundary layer may be long enough such that their chemical composition becomes dependent on the air mass history several days back in time. In order to get some idea on how this might affect our results, we made simulation in which one of the simulation days was either randomly removed from the whole simulation or repeated twice during the simulation.

The resulting changes in the submicron nss-SO_4 and MSA concentrations were up to 25% compared with the base-case simulation.

4. Conclusions

The MINOS campaign and the comprehensive dataset obtained during it gave us a unique opportunity to highlight the mechanisms of sulfur formation in the eastern Mediterranean. Two models, a chemical box model and an aerosol–cloud model have been synergistically applied to the data and then demonstrated that

- Gas-phase H_2SO_4 formation followed by condensation can fully explain submicron nss-SO_4 within the modeling and experimental uncertainties (roughly 30%).
- Only about 10% of the supermicron nss-SO_4 can be explained by condensation of gas-phase H_2SO_4, the rest must be formed via heterogeneous pathways.
- SO_2 oxidation by O_3 in wet sea-salt particles may explain the supermicron nss-SO_4 only if sea-salt particles have substantially (up to 30 times) higher alkalinity than present in natural sea water. Another possible pathway is nss-SO_4 formation on dust particles which account for the majority of supermicron mass.
- Condensation of gaseous MSA can explain particulate MS^- when MSA mass accommodation coefficient on particle surfaces is $\geqslant 0.3$. From the laboratory experiments available in the literature this is highly unlikely.
- Aqueous-phase oxidation of DMSO by OH can easily explain observed levels of particulate MS^-.
- Biogenic sulfur emissions contribute 5–20% of the measured total sulfur in the aerosol phase, a figure in agreement with earlier studies performed in the eastern Mediterranean.

Acknowledgements

HB thanks T. Elste and G. Stange for CIMS measurements during MINOS. K. Oikonomou is thanked for her help in IC analyses. We would like to thank the two anonymous reviewers for their insightful comments. This work has been supported by the Greek–French collaborative project, Platon.

References

Atkinson, R., Baulch, D.L., Cox, R.A., Crowley, J.N., Hampson, R.F., Hynes, R.G., Jenkin, M.E., Rossi, M.J., Troe, J., 2004. Evaluated kinetic and photochemical data for atmospheric chemistry: Volume I—gas phase reactions of O_x, HO_x, NO_x and SO_x species. Atmospheric Chemistry and Physics 4, 1461–1738.

Bardouki, H., Berresheim, H., Vrekoussis, M., Sciare, J., Kouvarakis, G., Oikonomou, K., Schneider, J., Mihalopoulos, N., 2003a. Gaseous (DMS, MSA, SO_2, H_2SO_4, and DMSO) and particulate (sulfate and methanesulfonate) sulfur species over the northeastern coast of Crete. Atmospheric Chemistry and Physics 3, 1871–1886.

Bardouki, H., Liakakou, H., Economou, C., Smolik, J., Zdimal, V., Eleftheriadis, K., Lazaridis, M., Mihalopoulos, N., 2003b. Chemical composition of size resolved atmospheric aerosols in the eastern Mediterranean during summer and winter. Atmospheric Environment 37, 195–208.

Barnes, I., Hjorth, J., Mihalopoulos, N., 2006. Dimethyl sulfide and dimethyl sulfoxide and their oxidation in the atmosphere. Chemical Reviews 106, 940–975.

Bates, T.S., Calhoun, J.A., Quinn, P.K., 1992. Variations in the methanesulfonate to sulfate molar ratio in submicrometer marine aerosol particles over the South Pacific Ocean. Journal of Geophysical Research 97, 9859–9865.

Berresheim, H., Plass-Dülmer, C., Elste, T., Mihalopoulos, N., Rohrer, F., 2003. OH in the coastal boundary layer of Crete during MINOS: measurements and relationship with ozone photolysis. Atmospheric Chemistry and Physics 3, 639–649.

Campolongo, F., Saltelli, A., Jensen, N.R., Wilson, J., Hjorth, J., 1999. The role of multiphase chemistry in the oxidation of dimethylsulphide (DMS). A latitude dependent study. Journal of Atmospheric Chemistry 32, 327–356.

Chameides, W.L., Stelson, A.W., 1992. Aqueous-phase chemical processes in deliquescent sea-salt aerosols: a mechanism that couples the atmospheric cycles of S and sea salt. Journal of Geophysical Research 97, 20565–20580.

De Bruyn, W.J., Shorter, J.A., Davidovits, P., Worsnop, D.R., Zahniser, M.S., Kolb, C.E., 1994. Uptake of gas phase sulfur species methanesulfonic acid, dimethylsulfoxide, and dimethyl sulfone by aqueous surfaces. Journal of Geophysical Research 99, 16927–16932.

Gerasopoulos, E., Koulouri, E., Kalivitis, N., Kouvarakis, G., Saarikoski, S., Makela, T., Hillamo, R., Mihalopoulos, N., 2007. Size-segregated mass distributions of aerosols over eastern Mediterranean: seasonal variability and comparison with AERONET columnar size-distributions. Atmospheric Chemistry and Physics 7, 2551–2561.

Gros, V., Williams, J., van Aardenne, J.A., Salisbury, G., Hofmann, R., Lawrence, M.G., von Kuhlmann, R., Lelieveld, J., Krol, M., Berresheim, H., Lobert, J.M., Atlas, E., 2003. Origin of anthropogenic hydrocarbons and halocarbons measured in the summertime european outflow (on Crete in 2001) Atmosphere. Chemical Physics 3, 1223–1235.

Herrmann, H., Ervens, B., Jacobi, H.-W., Wolke, R., Nowaki, P., Zellner, R., 2000. CAPRAM2.3: a chemical aqueous phase radical mechanism for tropospheric chemistry. Journal of Atmospheric Chemistry 36, 231–284.

Hoffman, M.R., 1986. On the kinetics and mechanism of oxidation of aquated sulfur dioxide by ozone. Atmospheric Environment 20, 1145–1154.

IPCC, 2001. Climate Change 2001. Intergovernmental Panel on Climate Change. Cambridge University Press, London.

Jefferson, A., Eisele, F.L., Ziemann, P.J., Weber, R.J., Marti, J.J., McMurry, P.H., 1997. Measurements of the H_2SO_4 mass accommodation coefficient onto polydisperse aerosol. Journal of Geophysical Research 102, 19021–19028.

Keene, W.C., Pszenny, A.A.P., Maben, J.R., Stevenson, E., Wall, A., 2004. Closure evaluation of size-resolved aerosol pH in the New England coastal atmosphere during summer. Journal of Geophysical Research 109, D23307.

Kerminen, V.-M., 2001. Relative roles of secondary sulfate and organics in atmospheric cloud condensation nuclei production. Journal of Geophysical Research 106, 17321–17333.

Kerminen, V.-M., Leck, C., 2001. Sulfur chemistry over the central Arctic Ocean during the summer: gas to particle transformation. Journal of Geophysical Research 106, 32,087–32,100.

Kerminen, V.-M., Virkkula, A., Hillamo, R., Wexler, A.S., Kulmala, M., 2000. Secondary organics and atmospheric cloud condensation nuclei production. Journal of Geophysical Research 105, 9255–9264.

Kouvarakis, G., Bardouki, H., Mihalopoulos, N., 2002. Sulfur budget above the eastern Mediterranean: relative contribution of anthropogenic and biogenic sources. Tellus 54, 201–213.

Kukui, A., Borissenko, D., Laverdet, G., Le Bras, G., 2003. Gas-phase reactions of OH radicals with dimethyl sulfoxide and methane sulfinic acid using turbulent flow reactor and chemical ionization mass spectrometry. Journal of Physical Chemistry A 107 (30), 5732–5742.

Kubilay, N., Koçak, M., Çokacar, T., Oguz, T., Kouvarakis, G., Mihalopoulos, N., 2002. The influence of Black sea and local biogenic activity on the seasonal variation of aerosol sulfur species in the eastern Mediterranean atmosphere. Global Biogeochemical Cycles, 16, 1029/2002GB001880.

Lee, Y.N., Zhou, X.L., 1994. Aqueous reaction-kinetics of ozone and dimethylsulfide and its atmospheric implications. Journal of Geophysical Research 99, 3597–3605.

Malm, W.C., Day, D.E., Kreidenweis, S.M., Collett Jr., J.L., Carrico, C., McMeeking, G., Lee, T., 2005. Hygroscopic properties of an organic-laden aerosol. Atmospheric Environment 39, 4969–4982.

Mihalopoulos, N., Stephanou, E., Kanakidou, M., Pilitsidis, S., Bousquet, P., 1997. Tropospheric aerosol ionic composition above the eastern Mediterranean Area. Tellus B, 314–326.

Moldanova, J., Ljungström, E., 2001. Sea-salt aerosol chemistry in coastal areas: a model study. Journal of Geophysical Research 106, 1271–1296.

Pöschl, U., Canagaratha, M., Jayne, J.T., Molina, L.T., Worsnop, D.R., Kolb, C.E., Molina, M.J., 1998. Mass accommodation coefficient of H_2SO_4 vapor on aqueous sulfuric acid surfaces and gaseous diffusion coefficient of H_2SO_4 in N_2/H_2O. Journal of Physical Chemistry A 102, 10082–10089.

Schwartz, S.E., Andreae, M.O., 1996. Uncertainty in climate change caused by anthropogenic aerosols. Science 272, 1121–1122.

Sciare, J., Bardouki, H., Moulin, C., Mihalopoulos, N., 2003. Aerosol sources and their contribution to the chemical composition of aerosols in the eastern Mediterranean sea during summertime. Atmospheric Chemistry and Physics 3, 291–302.

Sciare, J., Kanakidou, M., Mihalopoulos, N., 2000. Diurnal and seasonal variation of atmospheric dimethyl sulfoxide (DMSO) at Amsterdam island in the southern Indian ocean,. Journal of Geophysical Research 105, 17257–17265.

Sciare, J., Oikonomou, K., Cachier, H., Mihalopoulos, N., Andreae, M.O., Maenhaut, W., Sarda-Esteve, M., 2005. Aerosol mass closure and reconstruction of the light scattering coefficient over the eastern Mediterranean sea during the MINOS campaign. Atmospheric Chemistry and Physics 5, 2253–2265.

Seinfeld, J.H., Pandis, S.N., 1998. Atmospheric chemistry and physics: from air pollution to climate change. Wiley, Hoboken, NJ, 1360pp.

Shi, B., Seinfeld, J.H., 1991. On mass transport limitation to the rate of reaction of gases in liquid droplets. Atmospheric Environment 25A, 2371–2383.

Sievering, H., Cainey, J., Harvey, M., McCregor, J., Nichol, S., Quinn, P., 2004. Aerosol non-sea-salt sulfate in the remote marine boundary layer under clear-sky and normal cloudiness conditions: ocean-derived biogenic alkalinity enhances sea-salt sulfate production by ozone oxidation. Journal of Geophysical Research 109, D19317.

Slinn, S.A., Slinn, W.G.N., 1980. Predictions for particle deposition on natural waters. Atmospheric Environment 14, 1013–1016.

Tegen, I., Fung, I., 1994. Modeling of mineral dust in the atmosphere: sources, transport, and optical properties. Journal of Geophysical Research 99, 22897–22914.

Tsigaridis, K., Kanakidou, M., 2002. Importance of volatile organic compounds photochemistry over a forested area in central Greece. Atmospheric Environment 36 (19), 3137–3146.

Turpin, B.J., Lim, H.-J., 2001. Species contributions to PM2.5 mass concentrations: revisiting common assumptions for estimating organic mass. Aerosol Science and Technology 35, 602–610.

Vrekoussis, M., Kanakidou, M., Mihalopoulos, N., Crutzen, P.J., Lelieveld, J., Perner, D., Berresheim, H., Baboukas, E., 2004. Role of the NO_3 radicals in oxidation processes in the eastern Mediterranean troposphere during the MINOS campaign. Atmospheric Chemistry and Physics 4, 169–182.

Zhu, L., Nenes, A., Wine, P.H., Nicovich, J.M., 2006. Effects of organosulfur chemistry on particulate methanesulfonate to non-sea salt sulfate ratio in the marine boundary layer. Journal of Geophysical Research 111, D05316.